

Formation of disulphide linkages restricts intramolecular motions of fluorophore: Detection of molecular oxygen in food package

Sk. Atiur Rahaman, Dipon Kumar Mondal, Subhajit Bandyopadhyay*

*Department of Chemical Sciences, Indian Institute of Science Education and Research (IISER)
Kolkata, Mohanpur, Nadia 741246, India*

E-mail: sb1@iiserkol.ac.in

CONTENTS

1. General characterization	S2
2. Experimental details	S3-S5
2.1 Synthetic procedures	S3
2.2 NMR spectra	S4-S5
Figure S5. Absorption and emission spectra of compound 1	S6
Figure S6. Emission spectra of compound 1 in THF-H ₂ O mixtures	S6
Figure S7. Emission spectra of compound 1 in THF-H ₂ O mixtures at $\lambda_{\text{emission}} = 485$ nm	S7
3. General information of determination of quantum yield	S7
Figure S8. Emission spectra of compound 1 upon addition with H ₂ O ₂	S8
Figure S9. Emission spectra of compound 1 upon addition with I ₂	S8
Figure S10. Emission spectra of compound 1' upon addition with NaBH ₄	S9
Figure S11. Relative fluorescence intensity vs. partial pressure of oxygen	S9
4. General information of fluorescence lifetime analyses	S10
Figure S12. Chemical shift of ¹³ C NMR signals of compound 1 and polymer 1'	S10
5. General information of Advanced Polymer Chromatography (APC)	S10
Figure S13. SEM image	S11
Figure S14. Paper strip study	S11
6. A limit of detection	S12
Figure S15. Detection limit calculation pot	S12
7. Toxicity studies with mammalian cells: J774A.1	S12
Figure S16. Relative cell viability analysis	S13
S17. SCXRD structures of compound 2	S13
Crystallographic Details	S13
Table S2 . Crystallographic parameters.....	S14
Table S3 and Table S4 . Bond Lengths (Å) and Bond Angles (°) for 2	S15-S20

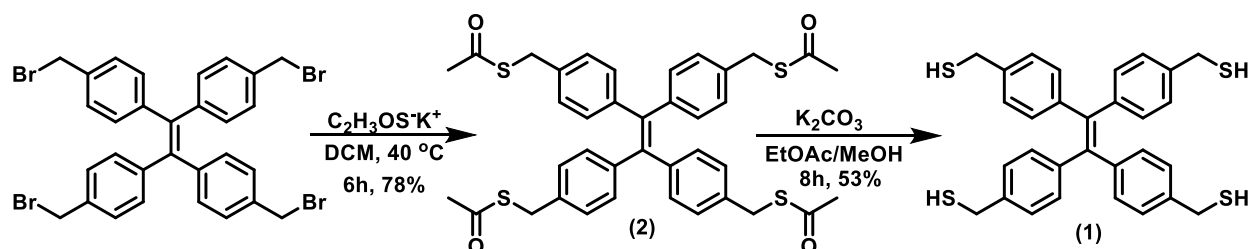
1. General characterization

All reactants and reagents were commercially available and were used without further purification unless otherwise indicated. Solvents used were purified and dried by standard methods. The structures of the compounds were determined by 1D and 2D NMR spectrometry and other spectroscopic techniques. ^1H and ^{13}C NMR spectra were recorded with 400 MHz JEOL and 500 MHz Bruker instruments. Chemical shifts are reported as δ values relative to an internal reference of tetramethylsilane (TMS) for ^1H NMR and the solvent peak in the case of ^{13}C NMR. The spectroscopic-grade solvents for the spectroscopic experiments were free from any fluorescent impurity. Double-distilled water was used for the spectroscopy experiments. UV-vis spectra were recorded with a Cary 60 UV-vis spectrophotometer. Fluorescence measurements were carried out with a JASCO FP-8500 Fluorescence Spectrometer (Xe-150 W, 200 - 750 nm). Fluorescence lifetime measurements were carried out by the method of time-correlated single-photon counting (TCSPC) using a picoseconds spectrofluorimeter from Horiba JobinYvon IBH equipped with a FluoroHub single photon counting controller, Fluoro3PS precision photomultiplier power supply, and FC-MCP-50SC MCP-PMT detection unit. The 402 nm laser head was used as the excitation source. Molecular weights and molecular weight distributions (dispersity (Đ)) of polymers were determined by Waters ACQUITY Advanced Polymer Chromatography (APC). MS data were obtained from an Acquity ultraperformance liquid chromatography (LC)-MS. Reactions were monitored by thin-layer chromatography (TLC) using Merck plates (TLC Silica Gel 60 F254). Developed TLC plates were visualized with UV light (254 nm). Silica gel (100–200 mesh, Merck) was used for column chromatography. Yields refer to the chromatographically and spectroscopically pure compounds.

2. Experimental details

2.1 Synthetic procedures

Scheme S1. Chemical structures and synthetic route .



The starting material 1,1,2,2-tetrakis(4-(bromomethyl)phenyl)ethene was prepared following the literature.¹

S,S',S'',S'''-((ethene-1,1,2,2-tetrayltetrakis(benzene-4,1-diyl))tetrakis(methylene))tetraethenethioate (2)

Potassium thioacetate (0.132 g, 0.5822 mmol) and 1,1,2,2-tetrakis(4-(bromomethyl)phenyl)ethene (0.1 g, 0.142 mmol) were dissolved in 15 mL of dichloromethane and was subsequently stirred for 6h at 40 °C. The volatiles were removed by rotary-evaporation at 35 °C. The crude product was washed with water and NaHCO_3 saturated solution and redissolved in dichloromethane, then, dried over sodium sulphate. The column chromatography performed using ethyl acetate/hexane (30:70, v/v) afforded **2** (0.076 g, 78%) as a white solid. mp 356–358 °C. ^1H NMR (500 MHz, CDCl_3) δ 2.34 (s, 3H), 4.03 (s, 2H), 6.89 (d, 2H, $J = 7.8$ Hz), 6.99 (d, 2H, $J = 8.1$ Hz). ^{13}C NMR (125 MHz, CDCl_3) δ 30.3, 33.2, 128.1, 131.4, 135.5, 140.2, 141.4, 198.1.

(Ethene-1,1,2,2-tetrayltetrakis(benzene-4,1-diyl))tetramethanethiol (1)

K_2CO_3 (0.097 g, 0.701 mmol) was added to compound **2** (0.1 g, 0.146 mmol) in 1:1 EtOAc/MeOH (6 mL) and the mixture was stirred for 8 h at 25 °C. After concentration, the residue was diluted with dichloromethane (10 mL) and H_2O (5 mL). The organic layer was dried over sodium sulphate. Column chromatography performed using ethyl acetate/hexane (20:80, v/v) afforded **1** (0.04 g, 53%) as a yellow solid. mp 345–347 °C. ^1H NMR (400 MHz, CDCl_3) δ 1.71 (t, 4H, $J = 7.64$ Hz), 3.67 (d, 8H, $J = 7.64$ Hz), 6.95 (d, 8H, $J = 8.4$ Hz), 7.06 (d, 8H, $J = 8.4$ Hz). ^{13}C NMR (125 MHz, CDCl_3) δ 33.3, 128.6, 131.6, 136.2, 140.6, 143.2. ESI-MS (m/z): Calcd. for $\text{C}_{30}\text{H}_{28}\text{S}_4$ [$\text{M}+\text{NH}_4$] $^+$ 534.1418, found 534.1417. Anal. Calcd. for $\text{C}_{30}\text{H}_{28}\text{S}_4$: C, 69.72; H, 5.46; S, 24.81, found: C, 69.68; H, 5.43; S, 24.78.

2.2 NMR spectra

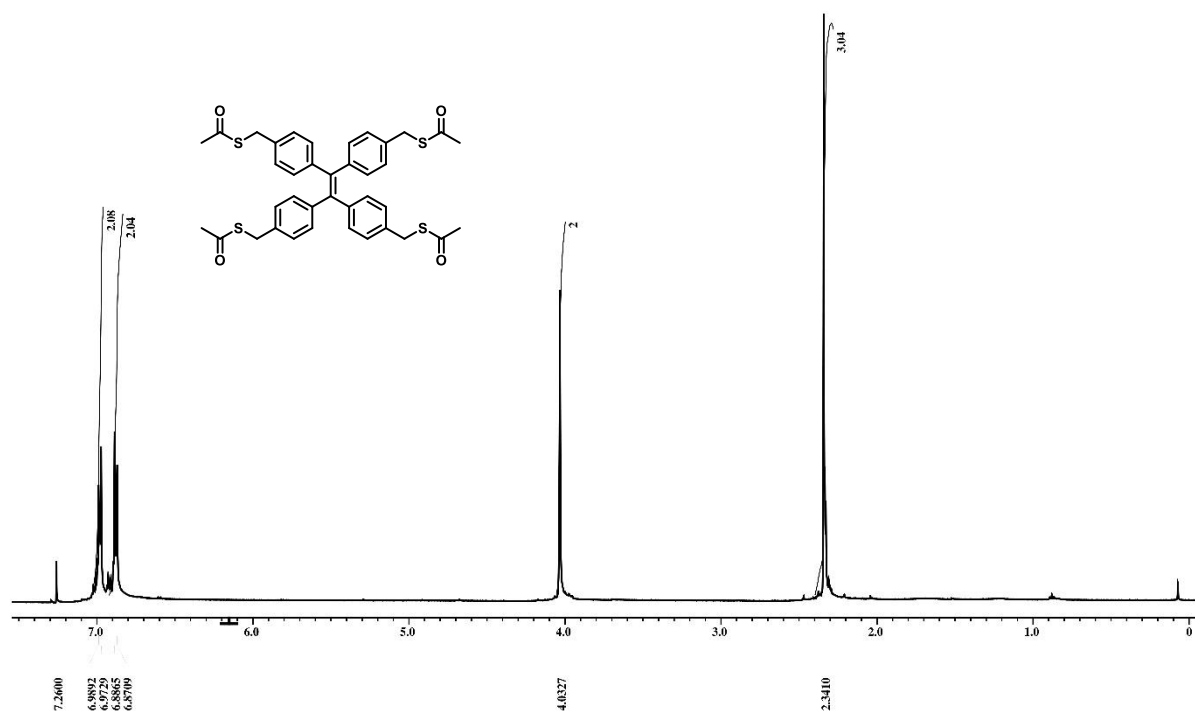


Figure S1. ¹H-NMR spectrum of compound 2

GROUP SB
SB-AR-8851 in CDCl₃

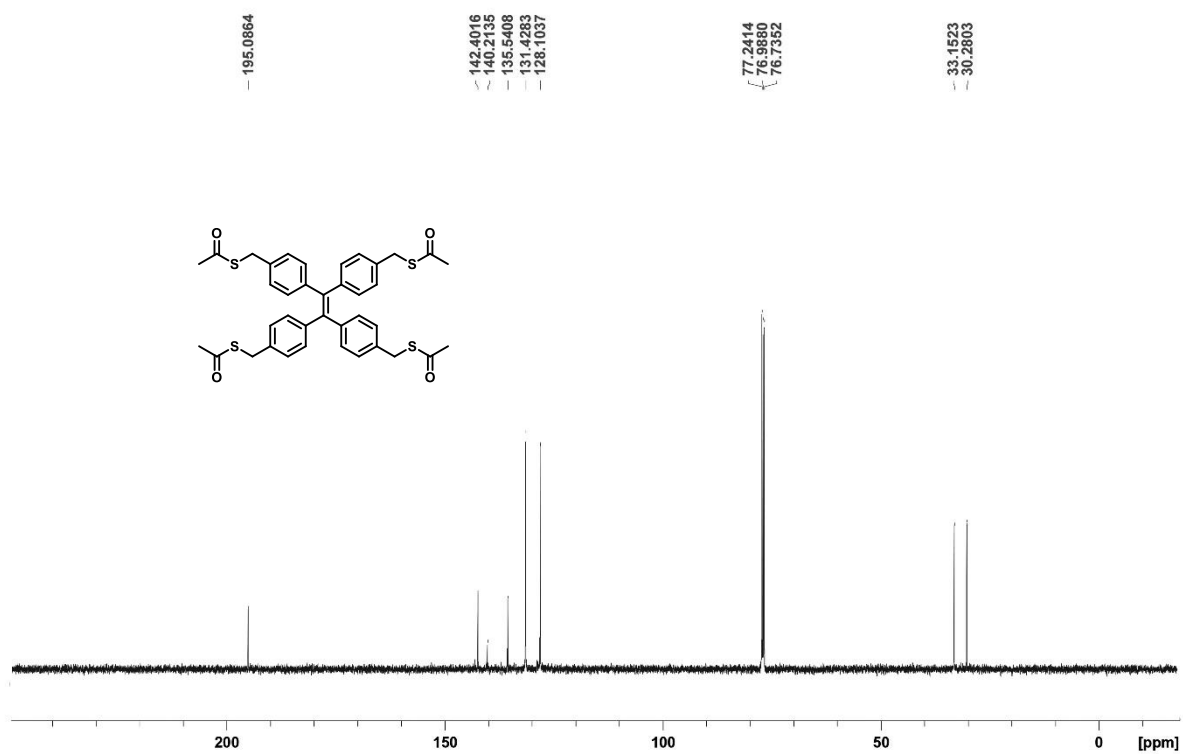


Figure S2. ^{13}C -NMR spectrum of compound **2**

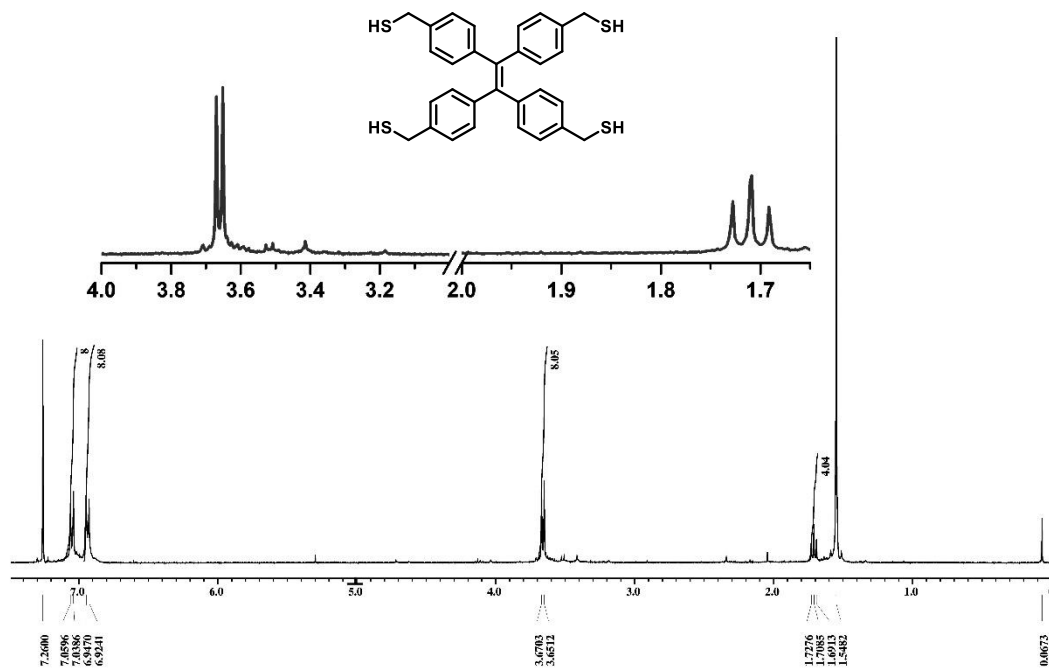


Figure S3. ^1H -NMR spectrum of compound **1**

GROUP SB
SB-AR-9851 in CDCl₃

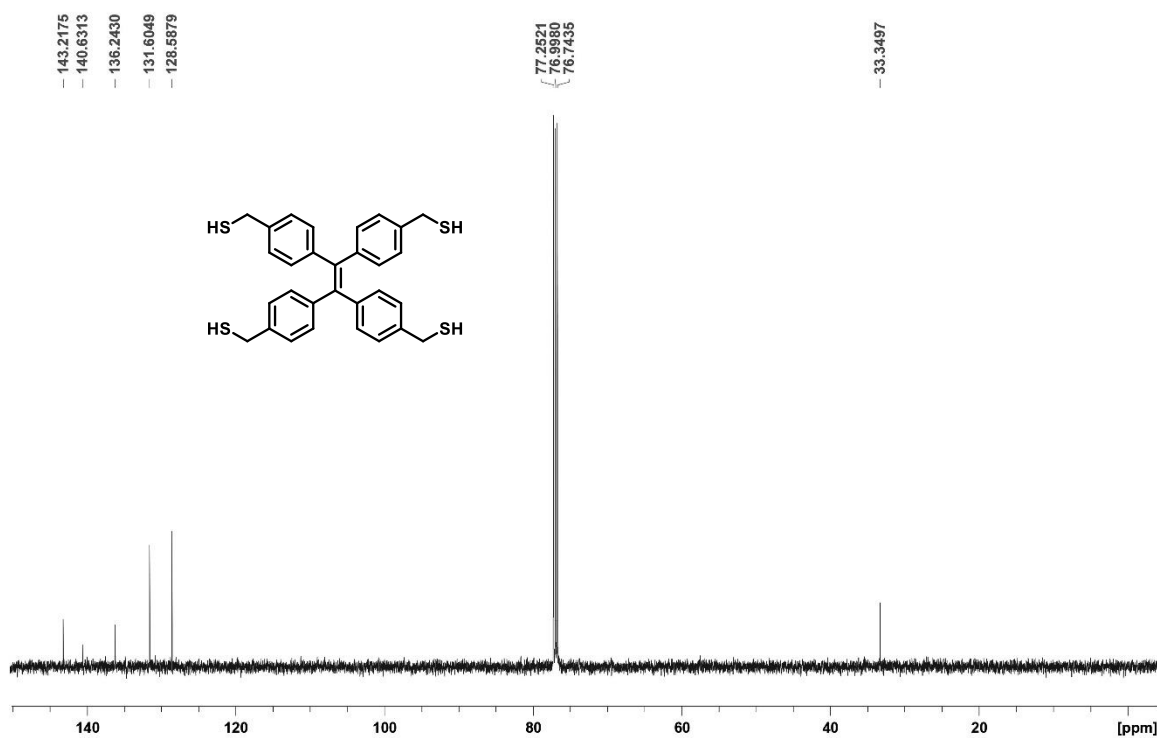


Figure S4. ^{13}C -NMR spectrum of compound **1**

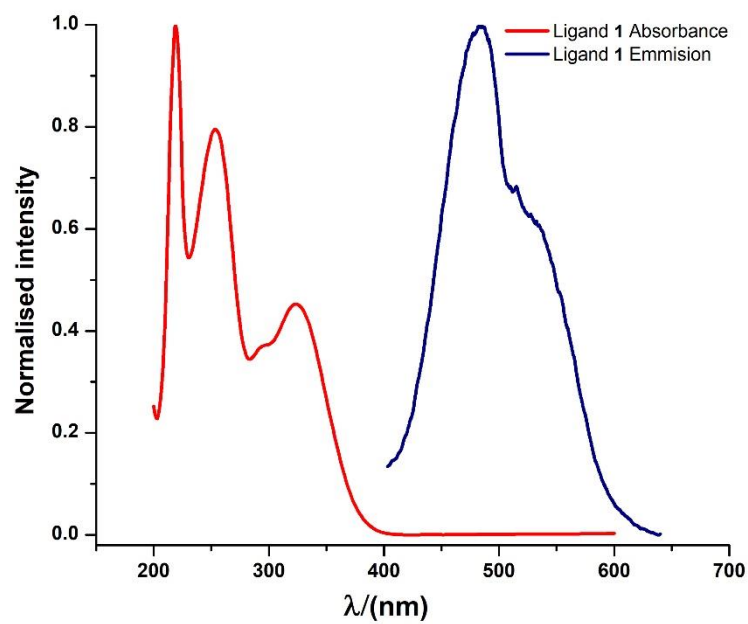


Figure S5. Electronic absorption and emission spectra ($\lambda_{\text{ex}} = 320$ nm, excitation and emission slit width 5/5) of compound **1** (10 μM) in THF media at 25 $^{\circ}\text{C}$.

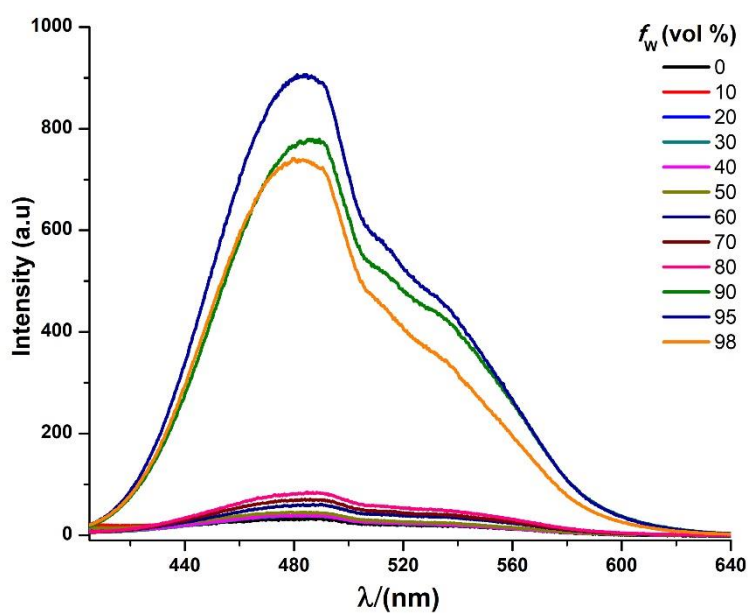


Figure S6. Emission spectra of compound **1** in THF–H₂O mixtures with different water fractions (f_w).

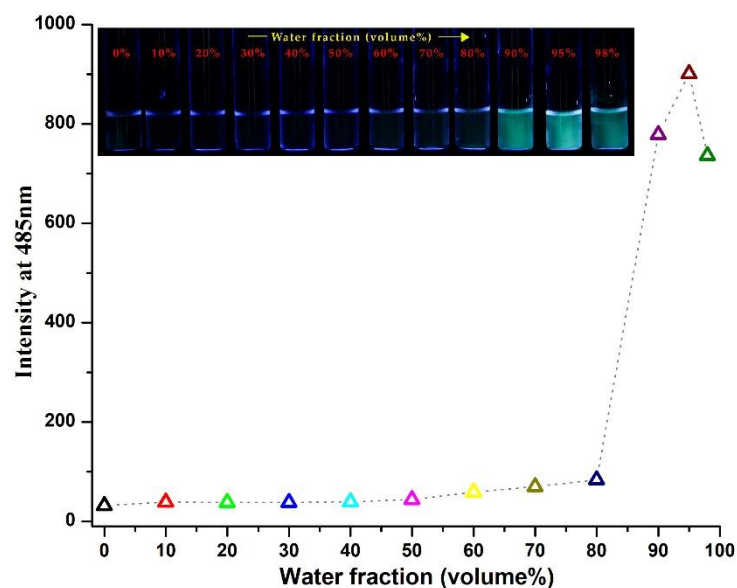


Figure S7. Plot of fluorescence intensity ($\lambda_{\text{emission}} = 485 \text{ nm}$) of **1** versus composition of THF/water mixture. Insert: Photographs of the solutions or suspensions of the molecules of **1** in THF/water mixtures with different volumetric fractions of water (f_w , vol%) under 366 nm light.

3. Determination of quantum yield²

The quantum yields (ϕ) of the compound **1** and polymer were calculated by comparing their integrated fluorescence intensities (excitation at 350 nm) and the absorbance values at 350 nm with those of quinine sulfate. Quinine sulfate ($\phi_s = 0.54$) was dissolved in 0.1M H_2SO_4 (refractive index: 1.33) and the compound **1** and polymer were dissolved in THF (refractive index: 1.407). The integrated fluorescence intensity is the area under the fluorescence curve in the wavelength range from 365 to 680 nm.

Relative quantum yield was calculated from the equation below:

$$\phi_F = \phi_S \cdot \frac{A_S}{A_U} \cdot \frac{F_U}{F_S} \cdot \frac{\eta_U^2}{\eta_S^2}$$

Where ϕ_s is the quantum yield of the standard, A is the absorbance at the excitation wavelength (subscript S for standard* and U for unknown), F is the area under the emission spectra and η is the refractive index of the solvent.

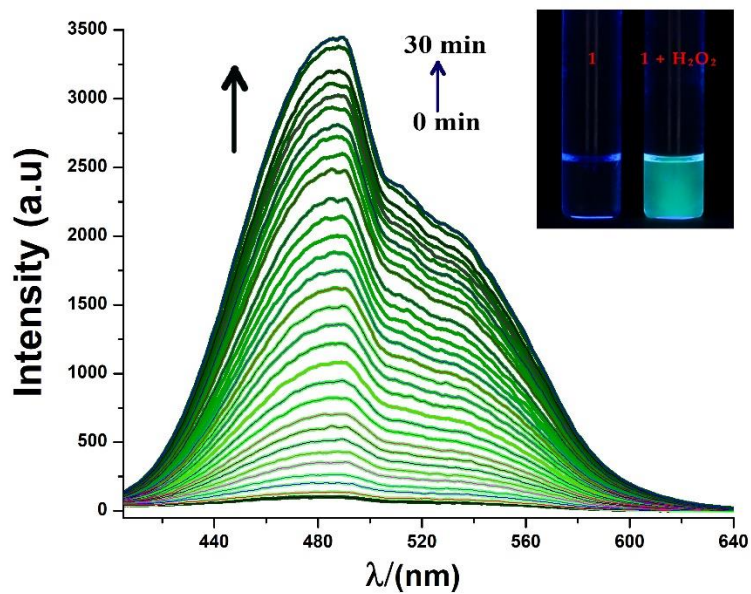


Figure S8. Changes in the emission spectra of compound **1** (10 μM) (λ_{ex} : 320 nm, slit: 5/5); Insert: visual change under 366 nm light in THF media at 25 $^{\circ}\text{C}$ upon addition with H_2O_2 (10 μM).

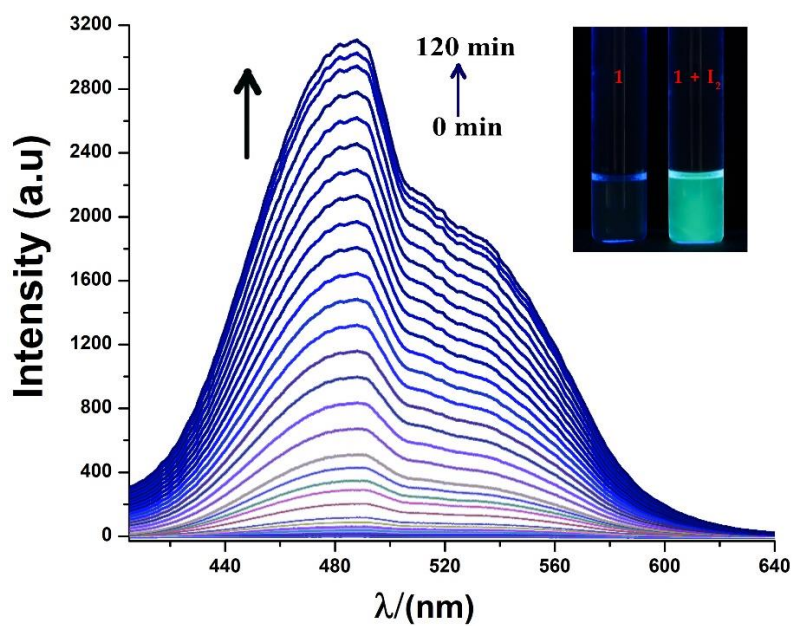


Figure S9. Changes in the emission spectra of compound **1** (10 μM) (λ_{ex} : 320 nm, slit: 5/5); Insert: visual change under 366 nm light in THF media at 25 $^{\circ}\text{C}$ upon addition with I_2 (10 μM).

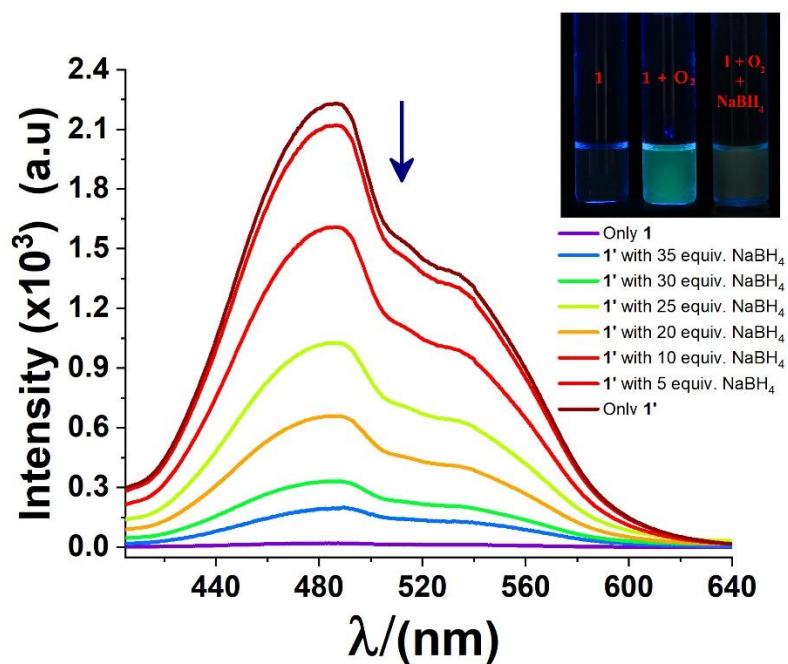


Figure S10. Changes in the emission spectra of polymer **1'** (10 μM) (λ_{ex} : 320 nm, slit: 5/5) studies for establishing the reversibility in binding of **1'** to NaBH_4 in THF media upon addition of 0-35 equivalents of BH_4^- at 25 $^\circ\text{C}$; Insert: visual changes under 366 nm UV light in THF media at 25 $^\circ\text{C}$ upon addition with BH_4^- .

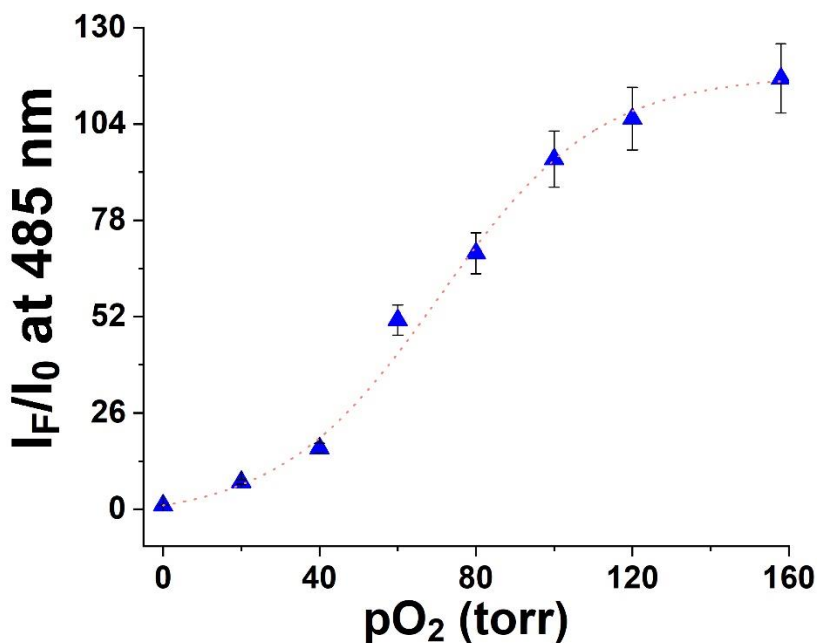


Figure S11. Relative fluorescence intensity vs. partial pressure of oxygen for compound **1** (10 μM) in THF media at 25 $^\circ\text{C}$ after 300 min.

4. Fluorescence lifetime analyses

The data in Fig. 3B was fitted with a biexponential decay equation:

$$I = \alpha_1 e^{-\frac{t}{\tau_1}} + \alpha_2 e^{-\frac{t}{\tau_2}}$$

The average lifetime $\langle\tau\rangle$ is given by:

$$\langle\tau\rangle = \frac{\alpha_1 \tau_1^2 + \alpha_2 \tau_2^2}{\alpha_1 \tau_1 + \alpha_2 \tau_2}$$

The TCSPC data has been presented in **Fig. 3B** (Main text).

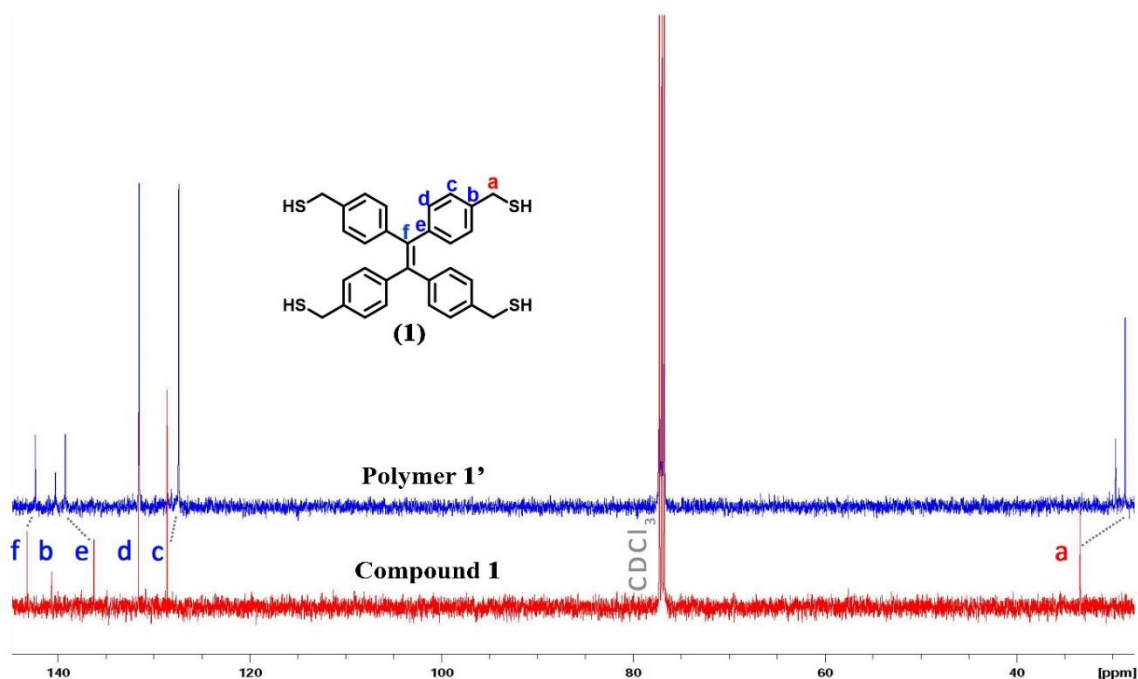


Figure S12. . The shift in the ^{13}C NMR signals of compound **1** upon bubbling with air.

Table S1 Delta shift value of ^{13}C NMR for compound **1** and polymer **1'**

Carbon	$(\delta_{\text{final}} - \delta_{\text{initial}}) = \Delta\delta$	Remarks
a	4.6	Upfield
b	3	Upfield
c	1.2	Upfield
d	0.1	Upfield
e	-3	Downfield
f	0.9	Upfield

5. Advanced Polymer Chromatography (APC)

Molecular weights and molecular weight distributions (dispersity (\bar{D})) of polymers were determined by Waters ACQUITY Advanced Polymer Chromatography (APC). The instrument contains a 1500 series HPLC pump, an ACQUITYTM refractive index (RI) detector, one ACQUITY APCTM XT

2002.5 μm (4.6×7.5 mm) column in THF at 45 $^{\circ}\text{C}$ at 0.25 mL/min flow rate. Poly(methyl methacrylate) (PMMA) standards were used to calibrate the instrument.

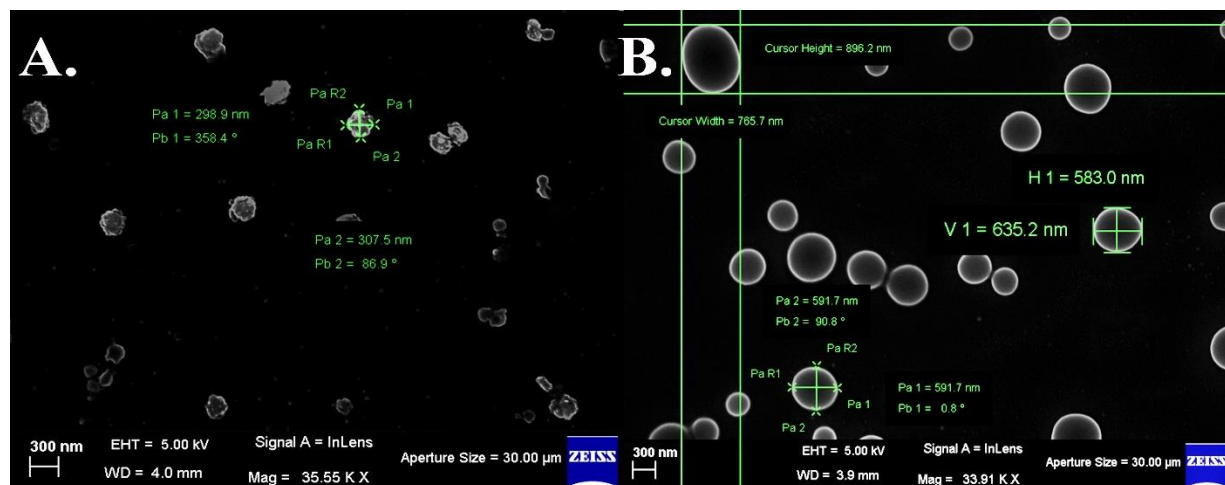


Figure S13. SEM image of a dried sample of compound **1** (A) and polymer **1'** (B).

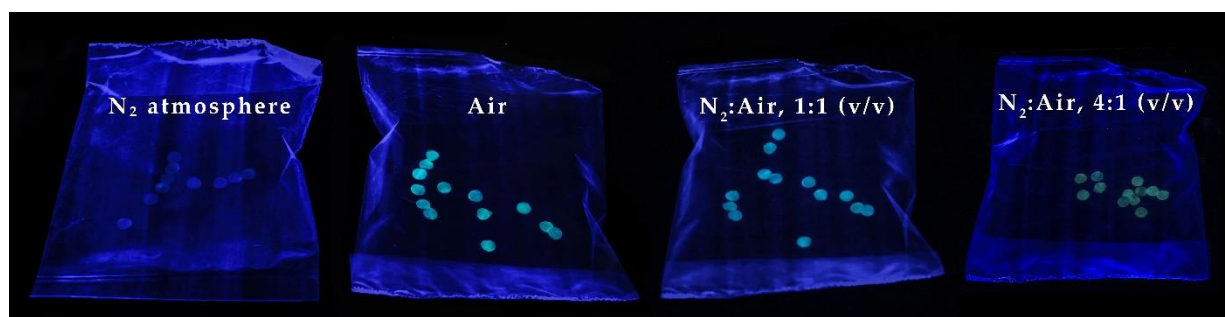


Figure S14. The photographs of the paper-dots of **1** (see the main text) in sealed plastic bags under various ratios of N₂ gas and atmospheric air after 2 days.

6. The limit of detection of oxygen in 24 h time scale upon exposure to O₂

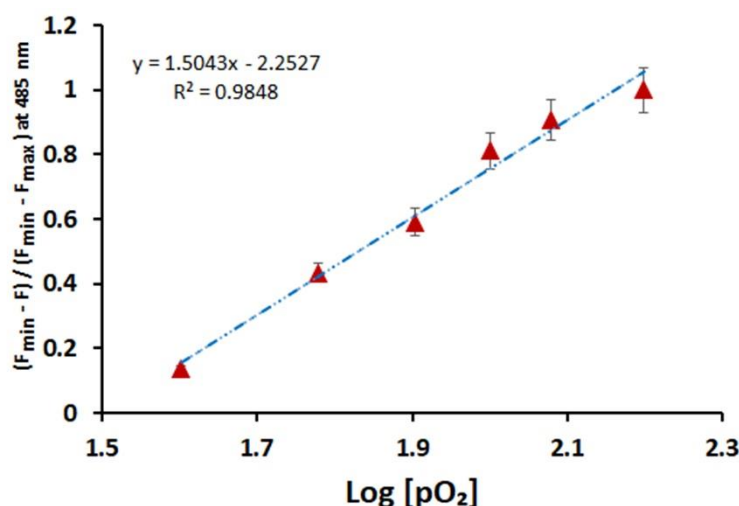


Figure S15. A linear curve was obtained from these normalized fluorescence intensity data. The intercept on the x-axis was considered as the detection limit. Thus the value obtained for the partial pressure of oxygen was found to be 30.8 torr.

7. Toxicity studies with mammalian cells: J774A.1

J774A.1 (murine macrophage cell line from the National Centre for Cell Science, Pune, India) cells were grown in Dulbecco's modified Eagle's medium (Gibco) supplemented with 2 mM L-glutamine, 100 µg/ml penicillin, 100 µg/ml streptomycin, and 10% heat-inactivated fetal bovine albumin (Gibco) at 37 °C in a humidified atmosphere containing 5% CO₂.

7.1 Analysis of cell viability after treatment with probe 1

The J774A.1 cells were treated with probe **1** at different concentrations (0.1 µM to 100 µM) as indicated in the X-axis of Figure S16. Each of the sets of the cell line was treated with the various concentrations of **1** for 24 hours. Control experiments under identical conditions in the absence of probe **1** was also studied. Equal amount of the cells from the control, and the sample treated with probe **1** were incubated with 0.5 mg/ml MTT [3-(4, 5-dimethylthiazol-2-yl)-2,5-diphenyl tetrazolium bromide] (Invitrogen) for 2 h to allow formation of purple formazan. Then the cells were washed with phosphate-buffered saline (PBS) and harvested by centrifugation, and the cell pellet was dissolved in DMSO. The optical density (OD) of the solution was measured on a microplate reader (SpectraMax M2e; Molecular Devices) at a wavelength of 595 nm. Since the

OD of formazan produced by the action of mitochondrial dehydrogenases of metabolically active cells correlates with the number of viable cells, the percentage of viability upon drug treatment was calculated using the formula ($OD_{\text{treated}}/OD_{\text{control}} \times 100$).

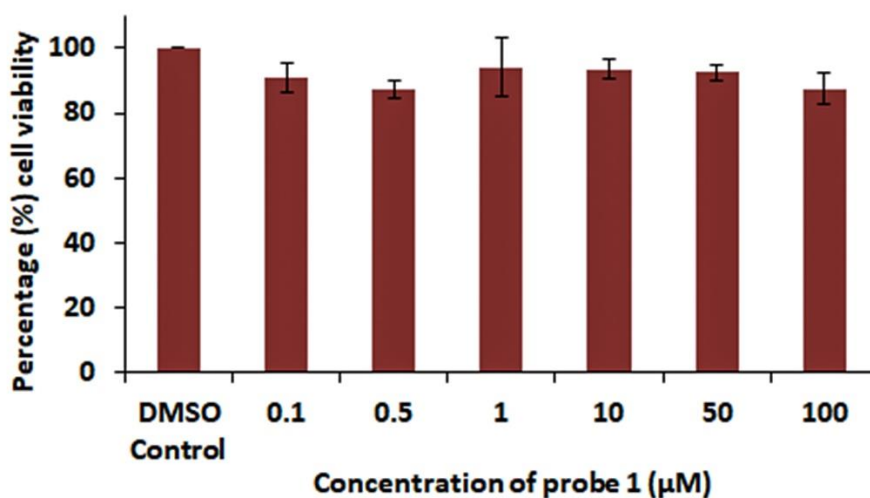


Figure S16. Relative cell viability analysis of J774A.1 murine macrophage cell line in different treatments after incubated for 24 h (errors were estimated from the std.dev. of three independent trials).

8. SCXRD structure

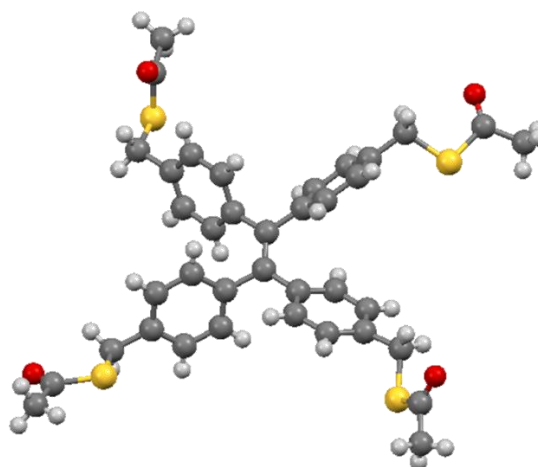


Figure S17. SCXRD structures of compound 2.

Crystallographic Details

Single crystals of $C_{38}H_{36}O_4S_4$ (CCDC Number 1879842) was obtained by slow diffusion of CH_2Cl_2 : hexane (1:1, v/v) solution. Suitable crystals for sample was selected on a SuperNova, Dual, Cu at zero, Eos diffractometer using graphite monochromatic Mo $K\alpha$ radiation ($\lambda = 0.71073 \text{ \AA}$). The crystals were kept at 100 K respectively during data collection. Using Olex³ the structures were

solved with the Super flip⁴ structure solution program using Charge Flipping and refined with the ShelXL⁵ refinement package using Least Squares minimisation. All hydrogen atoms were added according to the riding model. Crystallographic parameters for compound **1** is given in the **Table S1**. Selected bond lengths and bond angles of compound **1** are given in the **Table S2** and **Table S3**.

Table S2. Crystallographic parameters and structure refinements for **1**.

Chemical formula	C ₃₈ H ₃₆ O ₄ S ₄
M_r	684.91
Crystal system, space group	Monoclinic, $P2_1/n$
Temperature (K)	100
a, b, c (Å)	11.2605 (7), 28.0222 (14), 11.3063 (5)
β (°)	102.040 (5)
V (Å ³)	3489.2 (3)
Z	4
Radiation type	Mo $K\alpha$
μ (mm ⁻¹)	0.31
Crystal size (mm)	0.36 × 0.33 × 0.26
Data collection Diffractometer	SuperNova, Dual, Cu at zero, Eos
T_{\min} : T_{\max}	0.711, 1.000
No. of measured, independent and observed [$I > 2\sigma(I)$] reflections R_{int}	12229, 5886, 4863 0.042
$(\sin \theta/\lambda)_{\text{max}}$ (Å ⁻¹)	0.595
Refinement	
$R[F^2 > 2\sigma(F^2)]$, $wR(F^2)$, S	0.108, 0.309, 1.06
No. of reflections	5886
No. of parameters	419
H-atom treatment	H-atom parameters constrained
	$w = 1/[\sigma^2(F_o^2) + (0.1629P)^2 + 14.4689P]$ o where $P = (F_o^2 + 2F_c^2)/3$
$\Delta\rho_{\text{max}}$, $\Delta\rho_{\text{min}}$ (e Å ⁻³)	2.70, -1.01

Table S3. Bond Lengths (Å) for **2**.

Number	Atom1	Atom2	Length
1	S001	C00M	1.770(6)
2	S001	C011	1.824(6)
3	S002	C012	1.813(6)
4	S002	C013	1.777(7)
5	S003	C014	1.849(7)
6	S003	C018	1.767(9)
7	S004	C015	1.760(9)
8	S004	C019	1.769(9)
9	O005	C00M	1.194(7)
10	O006	C013	1.156(9)
11	O007	C015	1.17(1)
12	C008	C00B	1.483(7)
13	C008	C00C	1.384(7)
14	C008	C00D	1.398(8)
15	C009	C00A	1.409(8)
16	C009	C00B	1.493(7)
17	C009	C00K	1.379(8)
18	C00A	H00A	0.93
19	C00A	C00J	1.383(8)
20	C00B	C00G	1.371(7)
21	C00C	H00C	0.929
22	C00C	C00N	1.384(7)
23	C00D	H00D	0.93
24	C00D	C00U	1.376(8)
25	C00E	H00E	0.93
26	C00E	C00F	1.405(7)
27	C00E	C00S	1.380(8)
28	C00F	C00G	1.478(8)
29	C00F	C00T	1.398(8)
30	C00G	C00H	1.501(7)
31	C00H	C00I	1.398(8)
32	C00H	C00P	1.397(9)
33	C00I	H00I	0.93
34	C00I	C00Q	1.394(8)
35	C00J	H00J	0.93
36	C00J	C00O	1.38(1)
37	C00K	H00K	0.93
38	C00K	C00R	1.387(8)
39	C00L	C00N	1.382(9)

40	C00L	C00U	1.405(9)
41	C00L	C012	1.518(8)
42	C00M	C00Y	1.504(8)
43	C00N	H00N	0.93
44	C00O	C00R	1.384(9)
45	C00O	C014	1.499(8)
46	C00P	H00P	0.931
47	C00P	C00W	1.394(8)
48	C00Q	H00Q	0.93
49	C00Q	C00V	1.39(1)
50	C00R	H00R	0.929
51	C00S	H00S	0.929
52	C00S	C00Z	1.403(8)
53	C00T	H00T	0.929
54	C00T	C010	1.378(8)
55	C00U	H00U	0.929
56	C00V	C00W	1.380(8)
57	C00V	C011	1.534(9)
58	C00W	H00W	0.929
59	O00X	C018	1.13(1)
60	C00Y	H00B	0.961
61	C00Y	H00F	0.96
62	C00Y	H00G	0.959
63	C00Z	C010	1.389(8)
64	C00Z	C019	1.52(1)
65	C010	H010	0.93
66	C011	H01A	0.97
67	C011	H01B	0.97
68	C012	H01C	0.971
69	C012	H01D	0.969
70	C013	C01A	1.48(1)
71	C014	H01E	0.97
72	C014	H01F	0.97
73	C015	C017	1.47(1)
74	C016	H01G	0.961
75	C016	H01H	0.96
76	C016	H01I	0.96
77	C016	C018	1.51(1)
78	C017	H01J	0.96
79	C017	H01K	0.96
80	C017	H01L	0.96
81	C019	H01M	0.97
82	C019	H01N	0.97
83	C01A	H01O	0.96

84	C01A	H01P	0.96
85	C01A	H01Q	0.96

Table S4. Bond Angles (°) for **2**.

Number	Atom1	Atom2	Atom3	Angle
1	C00M	S001	C011	100.0(3)
2	C012	S002	C013	101.4(3)
3	C014	S003	C018	98.3(4)
4	C015	S004	C019	103.5(4)
5	C00B	C008	C00C	118.7(5)
6	C00B	C008	C00D	124.0(5)
7	C00C	C008	C00D	117.2(5)
8	C00A	C009	C00B	118.5(5)
9	C00A	C009	C00K	118.4(5)
10	C00B	C009	C00K	123.1(5)
11	C009	C00A	H00A	120
12	C009	C00A	C00J	120.0(5)
13	H00A	C00A	C00J	120
14	C008	C00B	C009	113.2(4)
15	C008	C00B	C00G	124.3(5)
16	C009	C00B	C00G	122.5(5)
17	C008	C00C	H00C	118.9
18	C008	C00C	C00N	122.1(5)
19	H00C	C00C	C00N	119
20	C008	C00D	H00D	119.1
21	C008	C00D	C00U	121.7(5)
22	H00D	C00D	C00U	119.2
23	H00E	C00E	C00F	119.1
24	H00E	C00E	C00S	118.9
25	C00F	C00E	C00S	121.9(5)
26	C00E	C00F	C00G	122.2(5)
27	C00E	C00F	C00T	116.4(5)
28	C00G	C00F	C00T	121.4(5)
29	C00B	C00G	C00F	123.4(5)
30	C00B	C00G	C00H	119.9(5)
31	C00F	C00G	C00H	116.6(4)
32	C00G	C00H	C00I	122.4(5)
33	C00G	C00H	C00P	120.0(5)
34	C00I	C00H	C00P	117.6(5)
35	C00H	C00I	H00I	119.6
36	C00H	C00I	C00Q	120.8(5)

37	H00I	C00I	C00Q	119.5
38	C00A	C00J	H00J	119.3
39	C00A	C00J	C00O	121.5(5)
40	H00J	C00J	C00O	119.2
41	C009	C00K	H00K	119.7
42	C009	C00K	C00R	120.5(5)
43	H00K	C00K	C00R	119.7
44	C00N	C00L	C00U	118.8(6)
45	C00N	C00L	C012	120.6(5)
46	C00U	C00L	C012	120.5(5)
47	S001	C00M	O005	122.1(5)
48	S001	C00M	C00Y	113.7(4)
49	O005	C00M	C00Y	124.2(5)
50	C00C	C00N	C00L	120.2(5)
51	C00C	C00N	H00N	119.9
52	C00L	C00N	H00N	119.9
53	C00J	C00O	C00R	118.2(6)
54	C00J	C00O	C014	121.2(6)
55	C00R	C00O	C014	120.6(6)
56	C00H	C00P	H00P	119.5
57	C00H	C00P	C00W	120.9(5)
58	H00P	C00P	C00W	119.5
59	C00I	C00Q	H00Q	119.5
60	C00I	C00Q	C00V	121.1(5)
61	H00Q	C00Q	C00V	119.4
62	C00K	C00R	C00O	121.4(5)
63	C00K	C00R	H00R	119.3
64	C00O	C00R	H00R	119.3
65	C00E	C00S	H00S	119.5
66	C00E	C00S	C00Z	120.9(5)
67	H00S	C00S	C00Z	119.6
68	C00F	C00T	H00T	119.2
69	C00F	C00T	C010	121.5(6)
70	H00T	C00T	C010	119.2
71	C00D	C00U	C00L	120.0(6)
72	C00D	C00U	H00U	120
73	C00L	C00U	H00U	120
74	C00Q	C00V	C00W	118.1(6)
75	C00Q	C00V	C011	121.5(5)
76	C00W	C00V	C011	120.4(5)
77	C00P	C00W	C00V	121.3(6)
78	C00P	C00W	H00W	119.4
79	C00V	C00W	H00W	119.3
80	C00M	C00Y	H00B	109.5

81	C00M	C00Y	H00F	109.5
82	C00M	C00Y	H00G	109.5
83	H00B	C00Y	H00F	109.4
84	H00B	C00Y	H00G	109.4
85	H00F	C00Y	H00G	109.5
86	C00S	C00Z	C010	117.2(6)
87	C00S	C00Z	C019	119.7(6)
88	C010	C00Z	C019	122.9(6)
89	C00T	C010	C00Z	121.9(6)
90	C00T	C010	H010	119.1
91	C00Z	C010	H010	119
92	S001	C011	C00V	108.7(4)
93	S001	C011	H01A	109.9
94	S001	C011	H01B	110
95	C00V	C011	H01A	109.9
96	C00V	C011	H01B	110
97	H01A	C011	H01B	108.3
98	S002	C012	C00L	109.2(4)
99	S002	C012	H01C	109.8
100	S002	C012	H01D	109.8
101	C00L	C012	H01C	109.8
102	C00L	C012	H01D	109.9
103	H01C	C012	H01D	108.3
104	S002	C013	O006	121.8(6)
105	S002	C013	C01A	112.7(6)
106	O006	C013	C01A	125.4(8)
107	S003	C014	C00O	112.9(5)
108	S003	C014	H01E	109
109	S003	C014	H01F	109
110	C00O	C014	H01E	109
111	C00O	C014	H01F	109
112	H01E	C014	H01F	107.8
113	S004	C015	O007	121.5(7)
114	S004	C015	C017	113.3(6)
115	O007	C015	C017	125.0(8)
116	H01G	C016	H01H	109.4
117	H01G	C016	H01I	109.4
118	H01G	C016	C018	109.4
119	H01H	C016	H01I	109.5
120	H01H	C016	C018	109.5
121	H01I	C016	C018	109.6
122	C015	C017	H01J	109.4
123	C015	C017	H01K	109.5
124	C015	C017	H01L	109.5

125	H01J	C017	H01K	109.4
126	H01J	C017	H01L	109.5
127	H01K	C017	H01L	109.5
128	S003	C018	O00X	120.2(7)
129	S003	C018	C016	111.2(6)
130	O00X	C018	C016	128.6(8)
131	S004	C019	C00Z	114.2(6)
132	S004	C019	H01M	108.7
133	S004	C019	H01N	108.7
134	C00Z	C019	H01M	108.7
135	C00Z	C019	H01N	108.7
136	H01M	C019	H01N	107.7
137	C013	C01A	H01O	109.4
138	C013	C01A	H01P	109.4
139	C013	C01A	H01Q	109.5
140	H01O	C01A	H01P	109.5
141	H01O	C01A	H01Q	109.5
142	H01P	C01A	H01Q	109.5

Reference

1. Y. -X. Zhu, Z. -W. Wei, M. Pan, H. -P. Wang, J. -Y. Zhang and C. -Y. Su, *Dalton Trans.*, 2016, **45**, 943.
2. (a) D. F. Eaton, Luminescence Spectroscopy, in Hand-book of Organic Photochemistry, ed. Scaiano. J. C, CRC Press, Boca Raton, **1**, 1989; (b) M. L. Sheepwash, R. H. Mitchell, and C. Bohne, *J. Am. Chem. Soc.*, 2002, **124**, 4693.
3. O. V. Dolomanov, L. J. Bourhis, R. J. Gildea, J. A. K. Howard, H. Puschmann, *J. Appl. Cryst.*, 2009, **42**, 339341.
4. L. Palatinus, G. Chapuis, *J. Appl. Cryst.*, 2007, **40**, 786-790.
5. G. M. Sheldrick, *Acta Cryst.*, 2008, **A64**, 112-122.